Note on a paper by Omta et al. on sawtooth oscillations

A. C. Fowler

SeMA Journal
Boletin de la Sociedad Española de Matemática Aplicada

ISSN 1575-9822
Volume 62
Number 1

SeMA (2013) 62:1-13
DOI 10.1007/s40324-013-0005-2

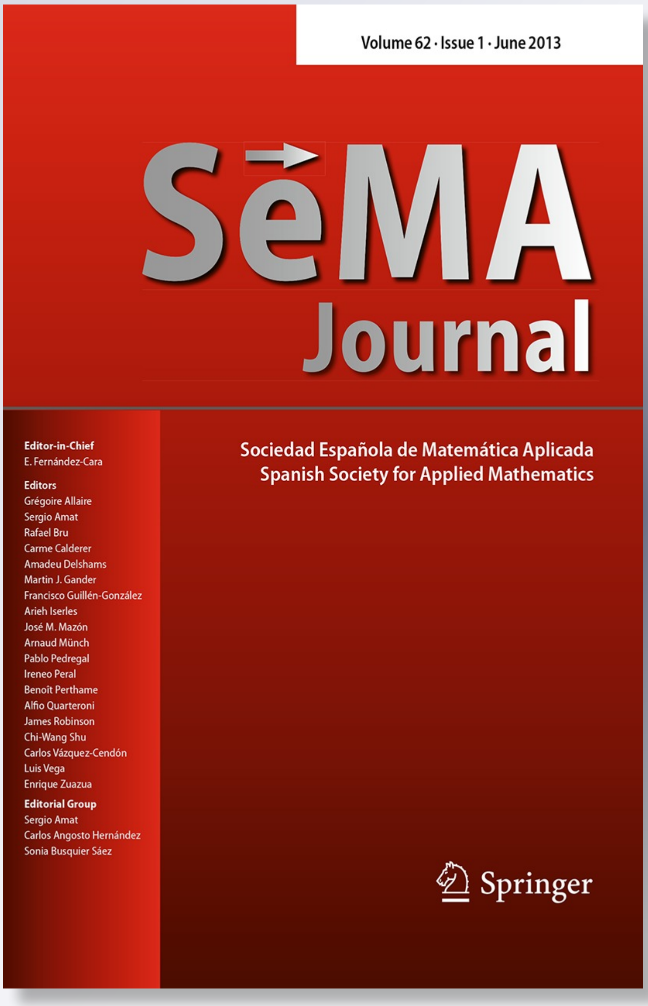

Springer

Your article is protected by copyright and all rights are held exclusively by Sociedad Española de Matemática Aplicada. This e-offprint is for personal use only and shall not be self-archived in electronic repositories. If you wish to self-archive your article, please use the accepted manuscript version for posting on your own website. You may further deposit the accepted manuscript version in any repository, provided it is only made publicly available 12 months after official publication or later and provided acknowledgement is given to the original source of publication and a link is inserted to the published article on Springer's website. The link must be accompanied by the following text: "The final publication is available at link.springer.com".

Springer

Author's personal copy

SeMA (2013) 62:1–13
DOI 10.1007/s40324-013-0005-2

Note on a paper by Omta et al. on sawtooth oscillations

A. C. Fowler

Received: 26 October 2012 / Accepted: 4 April 2013 / Published online: 22 May 2013
© Sociedad Española de Matemática Aplicada 2013

Abstract We discuss a recently proposed model for the sawtooth oscillations of atmospheric carbon observed in ice age cores. The model at its simplest arises from a single reaction involving just two species, oceanic biomass and nutrient, and bears similarity to models which have been proposed to explain oscillations in glycolysis. We show that the sawtooth behaviour, and associated spiking of one of the constituents, is associated with the existence of a conservative nonlinear oscillator with an asymmetric potential at high values of the energy, and we give asymptotic descriptions of the solutions. We extend the analysis to a more complicated model which includes competition between planktonic species.

Keywords Sawtooth oscillation · Ice ages · Carbon · Ocean biomass

Mathematics Subject Classification 86A10 · 86A40

1 Introduction

One of the most striking features of the climate of the last several million years is the occurrence of a regular sequence of ice ages, occurring over the last half million years with an approximate period of 100 ka (100,000 years), and with the interglacial periods between ice ages lasting roughly 10 ka. Since the last ice age terminated some 10 ka ago, we might be considered due for another one, except that the anthropogenic input of CO_2 into the atmosphere has altered the climatic prognosis dramatically.

The dramatic rôle of carbon in determining the Earth's mean temperature is highlighted in the time series shown in Fig. 1. The top graph represents variation of oxygen isotope ratio in benthic (deep ocean) sediments as a function of age (i. e., time goes from right to left) [11],

A. C. Fowler
MACSI, University of Limerick, Limerick, Ireland, UK

A. C. Fowler (✉)
OCIAM, University of Oxford, Oxford, UK
e-mail: fowler@maths.ox.ac.uk

Author's personal copy

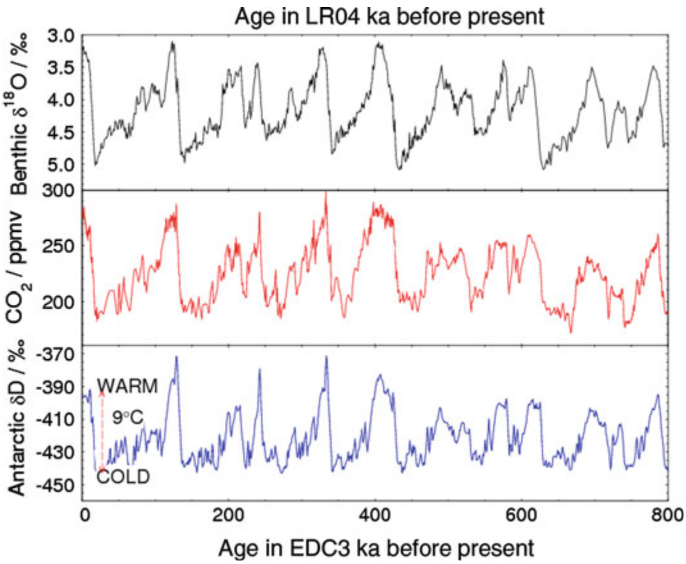

Fig. 1 Proxy temperature measurements from deep sea sediments (*top*), Antarctic ice core (*bottom*), and the CO_2 variation derived from the same Antarctic ice core

while the lower two curves show variation of CO_2 (middle) and deuterium ratio (lowest), taken from an Antarctic ice core [14]. The top and bottom curves are proxy measurements of temperature, and exhibit the sharp asymmetry of the ice age oscillations, while the middle curve shows that CO_2 follows the oscillations in temperature very closely. There has been some debate and interest in whether temperature leads CO_2 or vice versa [19], but for the present purpose, the important observation is that they are closely tied. Most obviously, temperature responds to CO_2 through the greenhouse effect, but also it is possible that CO_2 may respond to temperature via a number of mechanisms, the most obvious of which is the increased solubility of CO_2 in sea water at low temperatures.

From the mathematical point of view, there are at least two interesting features of the data shown in Fig. 1. The first is the synchronisation of carbon with temperature; the other is the asymmetrical saw-tooth nature of the oscillation, and it is with this that the present paper is concerned.

A popular view is that the cause of ice ages is due to the seasonal variation of the received summer insolation in northern latitudes. This is known as the Milanković theory, and was promoted by Croll [1,2] and Milanković [12]. The theory received strong support from the finding by Hays et al. [9] that the spectral signature of proxy data such as those in Fig. 1 was consistent with the various periods in the solar insolation curves, where frequencies of about 19, 23, 41 and 100 ka occur.

However, while it seems that the Milanković variations have an important influence on the ice age signal, data such as those in Fig. 2 suggests that the connection is far from obvious. In fact, Fig. 2 suggests that a more likely hypothesis is that the ice age oscillations represent those of a nonlinear oscillatory system driven by a quasi-periodic forcing. To this end, a number of authors have endeavoured to explain ice ages by means of relatively simple models which describe the interaction of the ice sheets with other components of the climate system.

Author's personal copy

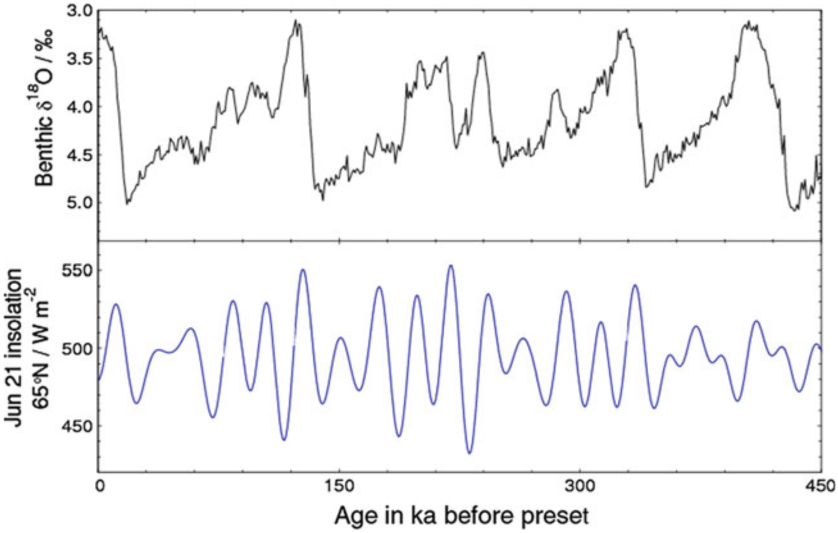

Fig. 2 Benthic oxygen isotopes [11] and an insolation curve for 65° north on June 21st [10] for the last 450 ka

Foremost amongst such models is the work by Saltzman [16–18]. The book by Saltzman [15] gives a voluminous summary of the efforts to build simple but realistic climate models which exhibit sawtooth oscillations, but the conclusion is not entirely satisfactory.

More recently, Fowler et al. [7] have developed an elaborate, but conceptually simple model, which is able to provide self-sustained sawtooth oscillations which simultaneously allow carbon to follow the temperature. Their model is constructed in a logical manner in order to fit the dynamical constraints imposed by Figs. 1 and 2. The essence of the matter is the sawtooth oscillation, and they are led to propose an active rôle for oceanic carbon, oceanic biomass and proglacial lakes. The last provide the vehicle for rapid deglaciation due to the rapid ice sheet wastage rates which are consequent on proglacial lake formation.

Omta et al. [13] propose a related, but simpler mechanism, which provides a mechanism for sawtooth oscillations. While they are motivated by the sawtooth oscillations in Fig. 1, their model does not explicitly include a description of ice sheet growth and decay. Its application to the observation is therefore worthy of further scrutiny. Crucifix [3] provides a thorough discussion of a number of other simple models of paleoclimate and their dynamical system structure.

The purpose of the present paper is not principally that of examining the scientific credibility of Omta et al.'s hypothesis, but rather to study their model with a view to explaining the origin of the sawtooth oscillations which they obtain. The point is, that sawtooth oscillations are not so easy to produce. The simplest relaxation oscillations of a second order pair of ordinary differential equations involve two rapid switches. It seems that the most obvious ingredients to produce a sawtooth oscillation (with a single rapid switch) would involve a three variable system, in which two slow variables migrate round a cusp catastrophe surface, with the other fast variable enabling the rapid transition. However, Omta et al.'s model is, in its essence, a two-dimensional model; it is this which drives our curiosity.

In this paper we show how the simplest version of the Omta model can be analysed, and we show how the sawtooth oscillations arise. In so doing, we also demonstrate that the oscillations are not sustained. The analysis is then extended to a four variable competition

Author's personal copy

Table 1 Values assumed for the simple model (2.3)

Symbol	Meaning	Typical value
I	Alkalinity input	0.8×10^{-3} eq m^{-3} ka-1
k	Reaction rate constant	50 m^{3} eq^{-1} ka^{-1}
S	Burial rate	10^{2} ka^{-1}
Y	Yield coefficient	$O(1)$ mol eq^{-1}

The unit eq (equivalent) is essentially the same as the mole

model, which forms the centrepiece of Omta et al.'s analysis, but we show that it can be analysed in the same way. In the conclusion we offer some comments on the applicability of Omta et al.'s results to the practical problem of paleoclimate explanation.

2 A simple model

Omta et al. [13] are motivated by the sawtooth oscillator of the ice ages, and the fact that carbon follows the same pattern. The simplest explanation for this is that in fact the ice ages are driven by oscillations in carbon, and to this end they analyse a model for carbon dynamics in the ocean, which is the principal controller for atmospheric carbon on time scales longer than a century [7].

The essence of the dynamics of carbon in the ocean is that it is is supplied by riverine input as bicarbonate, following weathering of silicate rocks. In the ocean, carbon is taken up by biomass such as coccolithophores which form calcium carbonate shells, and these are subsequently buried in benthic sediments, and thus removed from the system.

In the simplest form, Omta et al.'s model describes the interaction between ocean carbon, represented by the carbonate alkalinity

$$A = \left[\mathrm{HCO}_3^-\right] + 2\left[\mathrm{CO}_3^{2-}\right] \tag{2.1}$$

and the calcifying biomass P, based on the simple first order reaction

$$\xrightarrow{I} A + P \xrightarrow{k'} rP \xrightarrow{S} . \tag{2.2}$$

The input I represents the supply of alkalinity by weathering, and the plankton are removed by burial, with rate coefficient S. This model assumes autocatalytic production of the planktonic population, and is similar to models proposed to explain oscillatory behaviour in glycolysis [8], which exhibit sawtooth and spiking behaviour.

In a well-stirred medium, the reaction (2.2) can be modelled by the pair of ordinary differential equations

$$\begin{aligned} \dot{A} &= I - \frac{k}{Y} AP, \\ \dot{P} &= kAP - SP, \end{aligned} \tag{2.3}$$

where we define $r = 1 + Y$ and $k = k'Y$. Omta *et al* use values similar to those given in Table 1 and show that A has sawtooth oscillations, while P has spiking behaviour, as shown in Fig. 3. Our interest is to explain the nature of these oscillations.

Author's personal copy

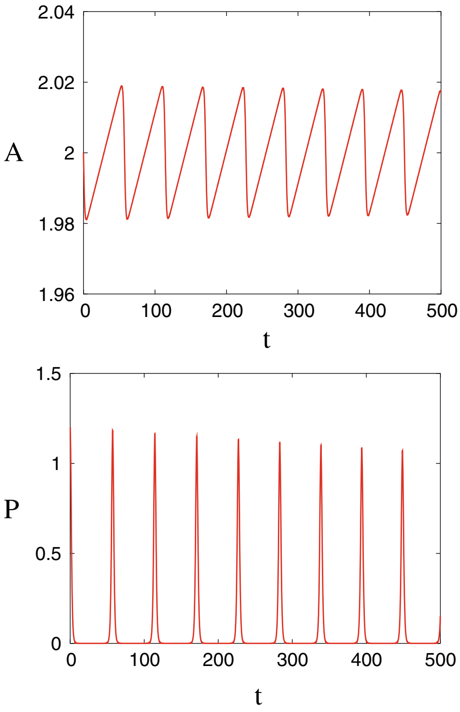

Fig. 3 Solution of (2.3) using the parameters in Table 1 (and $Y = 1$ eq mol^{-1}), so that $A_0 = 2$ eq m^{-3}, $P_0 = 0.8 \times 10^{-5}$ mol m^{-3} and $t_0' = 5$ ka. The time axis is in ka, that for A in eq m^{-3}, and that for P in 10^{-4} mol m^{-3}. The initial values were taken as $a = 0$ and $p = 15$, corresponding to $A = 2$ eq m^{-3} and $P = 1.2 \times 10^{-4}$ mol m^{-3}

Table 2 Values of the scales and the dimensionless parameter δ in (2.4), (2.5) and (2.9)

Symbol	Typical value
A_0	2 eq m^{-3}
P_0	0.8×10^{-5} mol m^{-3}
t_0	2.5×10^3 ka
t_0'	5 ka
δ	2×10^{-3}

The numerical results provide some help in determining the scaling. We choose scales A_0, P_0 and t_0 for A, P and t, where

$$A_0 = \frac{S}{k}, \quad P_0 = \frac{IY}{S}, \quad t_0 = \frac{S}{kI}; \tag{2.4}$$

typical values of these are given in Table 2. The dimensionless equations can then be written in the form

$$\begin{aligned} \dot{A} &= 1 - AP, \\ \delta^2 \dot{P} &= (A - 1)P, \end{aligned} \tag{2.5}$$

Author's personal copy

where

$$\delta = \frac{\sqrt{kI}}{S}. \tag{2.6}$$

For the values in Table 1, $\delta = 2 \times 10^{-3}$. Because $\delta \ll 1$, we rescale A and t by putting

$$A = 1 + \delta a, \quad t \sim \delta, \tag{2.7}$$

and the rescaled equations take the form

$$\begin{aligned} \dot{a} &= 1 - p(1 + \delta a), \\ \dot{p} &= ap, \end{aligned} \tag{2.8}$$

where we write $P = p$ for clarity. The time scale corresponding to this dimensionless time is

$$t_0' = \frac{1}{\sqrt{kI}}, \tag{2.9}$$

and has the value of 5 ka. Note that the period of the oscillations in Fig. 3 is about 70 ka, i. e., 14 in dimensionless terms.

It is now simple to provide an explanation for the spiking p and sawtooth A oscillations shown in Fig. 3. We define

$$\theta = \ln p, \tag{2.10}$$

and thus

$$a = \dot{\theta}, \tag{2.11}$$

and θ satisfies the damped nonlinear oscillator equation

$$\ddot{\theta} + V'(\theta) = -\delta \dot{\theta} e^{\theta}, \tag{2.12}$$

where the potential is

$$V(\theta) = e^{\theta} - \theta. \tag{2.13}$$

If we ignore the small damping term in δ, then there is a first integral

$$\tfrac{1}{2}\dot{\theta}^2 + V(\theta) = E, \tag{2.14}$$

and the asymmetry of the oscillations which produces the sawtooth and spiking is due to the strong asymmetry of the potential when E is large. The value of E is determined by the initial conditions, and in fact (2.12) shows that

$$\dot{E} = -\delta \dot{\theta}^2 e^{\theta}, \tag{2.15}$$

so that E relaxes to 0 (thus $p \to 1, a \to 0$ and $A \to 1$) over the long time scale $t \sim \frac{1}{\delta}$, corresponding to a time $t_0 = 2{,}500$ ka.

When E is large, we can give an asymptotic description of the solution. Again we put $\delta = 0$. Then θ oscillates between its maximum θ_+ and its minimum θ_-, where $V = E$, and these are given by

Author's personal copy

$$\theta_+ = \ln(E + \theta_+), \quad \theta_+ \approx \frac{E \ln E}{E - 1},$$
$$\theta_- = -\left[E - e^{\theta_-}\right], \quad \theta_- \approx -E + e^{-E}. \tag{2.16}$$

The spike in p occurs near the maximum of θ, where we define

$$\theta = \theta_+ + \phi, \quad t = \sqrt{\omega} T, \quad \omega = e^{-\theta_+} \ll 1, \tag{2.17}$$

and ϕ satisfies

$$\phi_{TT} + e^{\phi} = \omega. \tag{2.18}$$

Ignoring ω and taking the time origin at the maximum, the solution is

$$\phi = -2 \ln \cosh\left(\frac{T}{\sqrt{2}}\right), \tag{2.19}$$

and at large T,

$$\phi \sim -\sqrt{2} T + 2 \ln 2. \tag{2.20}$$

The approximation becomes invalid at large T, when the exponential becomes negligible. To find a suitable time scale, we define

$$\theta = \Lambda \Theta, \quad T = \Lambda \tau, \tag{2.21}$$

where $\Lambda \gg 1$, and thus to match to (2.19), we have

$$\Theta \sim \frac{\theta_+ + 2 \ln 2}{\Lambda} - \sqrt{2}\tau \tag{2.22}$$

as $\tau \to 0$. To balance terms, we choose

$$\Lambda = \frac{1}{\omega} = e^{\theta_+}, \tag{2.23}$$

and then

$$\Theta_{\tau\tau} - 1 + e^{\Lambda\Theta} = 0, \tag{2.24}$$

and the last term is negligible since $\Theta < 0$. The solution of this is then

$$\Theta = (\theta_+ + 2 \ln 2) e^{-\theta_+} - \sqrt{2}\tau + \tfrac{1}{2}\tau^2, \tag{2.25}$$

and this takes us all the way to the next maximum. The minimum occurs at $\tau = \sqrt{2}$, which thus gives half the period. The period in τ is thus $2\sqrt{2}$, and in terms of the original time t, it is $2\sqrt{2}e^{\theta_+/2}$, and in dimensional terms, the period is

$$P_{\text{dim}} \approx 2\left[\frac{2(E + \theta_+)}{kI}\right]^{1/2} \approx 2\left[\frac{2(E + \ln E)}{kI}\right]^{1/2}. \tag{2.26}$$

In summary, we have in dimensional terms, the peak of P is

$$P_{\max} = \frac{IYe^{\theta_+}}{S} \approx \frac{IY(E + \ln E)}{S}, \tag{2.27}$$

Author's personal copy

Table 3 Values of the parameters assumed for the four equation model (3.1)

Symbol	Typical value
F_A	0.9
F_N	1 mol mol^{-1}
h_1	39.98 year^{-1}
h_2	40 year^{-1}
I	0.8×10^{-5} eq m^{-3} year^{-1}
K_A	0.2 eq m^{-3}
K_N	0.5×10^{-3} mM
R	1 eq mol^{-1}
Y	1 mol mol^{-1}
μ_M	200 year^{-1}

while the minimum is

$$P_{\min} = \frac{IYe^{\theta_-}}{S} \approx \frac{IYe^{-E}}{S}; \tag{2.28}$$

the amplitude of the oscillation in A about the mean value is

$$A_0 \pm A_0\delta\Delta a \approx \frac{S}{k} \pm \sqrt{\frac{I}{k}}(E + \ln E), \tag{2.29}$$

and the period is given in (2.26).

3 A competition model

Omta et al. [13] also study an enhanced version of that discussed above, in which two species of plankton (calcifiers and non-calcifiers) compete for rate-limiting nutrient N, and they show that it has the same sawtooth oscillations. We now analyse a simple version of their model using the guidelines established for the two species model.

The Omta four-dimensional model is in effect the following:

$$\begin{aligned}
\dot{A} &= I - R(\mu_1 - F_A h_1)P_1, \\
\dot{P}_1 &= (\mu_1 - h_1)P_1, \\
\dot{P}_2 &= (\mu_2 - h_2)P_2, \\
\dot{N} &= \left(-\frac{\mu_1}{Y} + F_N h_1\right) P_1 + \left(-\frac{\mu_2}{Y} + F_N h_2\right) P_2,
\end{aligned} \tag{3.1}$$

and the coefficients μ_i are given by

$$\mu_1 = \frac{\mu_M}{1 + \frac{K_N}{N} + \frac{K_A}{A} - \frac{1}{\frac{N}{K_N} + \frac{A}{K_A}}}, \quad \mu_2 = \frac{\mu_M}{1 + \frac{K_N}{N}}. \tag{3.2}$$

This form of the model was used in Omta et al.'s original submitted paper. In the revised version, the model is elaborated by replacing carbonate alkalinity A in the definition of μ_1 with the carbonate ion concentration

Author's personal copy

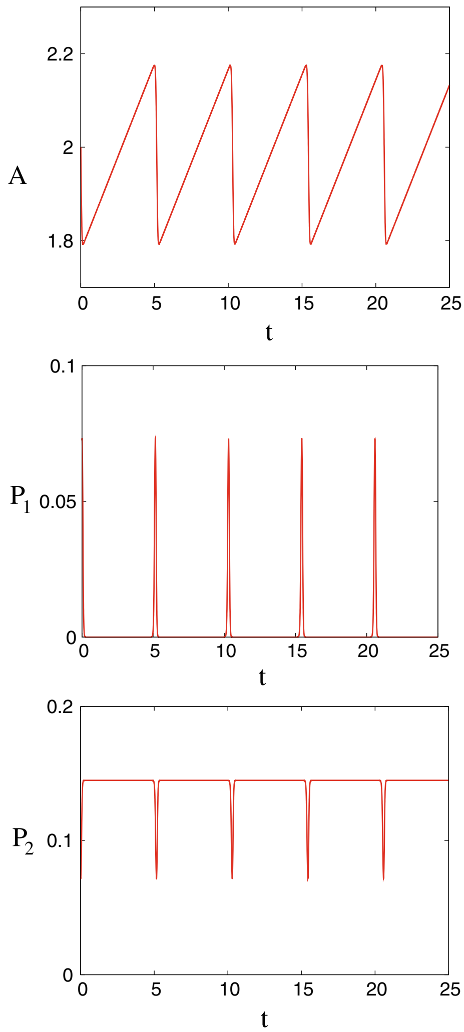

Fig. 4 Numerical solution of the four equation model (3.1) for the parameter values shown in Table 3, and with the constant K in (3.8) being $K = 2.16$. As explained in the text, N is almost constant after an initial transient. Here we have taken the initial value of N to be N_0 ($N = 1$ dimensionlessly), thus eliminating this transient. The units are 10^4 year for t, eq m^{-3} for A, and μM for P_1

$$S = \left[\mathrm{CO}_3^{2-}\right], \tag{3.3}$$

which is then related algebraically to A. In addition, they allow for different ocean compartments. We will proceed with (3.1) and (3.2) as they stand, since the difference is irrelevant to our central point, which is that (3.1) and (3.2) can be analysed in an essentially similar way to the simpler model (2.3).

We use the parameter values given in Table 3, for which a numerical solution is shown in Fig. 4. We see that A and P_1 have essentially the same behaviour, while P_2 resembles a constant minus P_1, and the nutrient N is virtually constant. Using these estimates for the solution, we can examine the sizes of the terms in μ_i, and this leads us to a choice of scaling analogous to that of the simple model which also determines the size of the scales. The procedure is a bit convoluted, so we simply give the resulting recipe.

Author's personal copy

Table 4 Values of the scales and dimensionless parameters for the four equation model (3.1)

Symbols	Typical value
A_0	2 eq m^{-3}
N_0	0.125×10^{-3} mM
P_0	2×10^{-6} mM
t_0	2.5×10^5 year
δ	10^{-2}
ε	0.5×10^{-3}
κ	0.2
ν	10^{-7}
σ	1.6×10^{-2}
ω	1.6×10^{-7}

We define two dimensionless parameters

$$\kappa = \frac{h_2}{\mu_M}, \quad \varepsilon = \frac{h_2 - h_1}{h_2}, \tag{3.4}$$

and then we choose scales A_0, P_0, N_0 and t_0 for A, P_i, N and t, where

$$N_0 = \frac{\kappa K_N}{1-\kappa}, \quad t_0 = \frac{A_0}{I}, \quad P_0 = \frac{I}{Rh_2(1-F_A)}, \quad A_0 = K_A \left(\frac{N_0 \kappa}{K_N \varepsilon} \right)^{1/2}, \tag{3.5}$$

and these have the typical values shown in Table 4.

The resulting non-dimensional form of the Eq. (3.1) is then

$$\begin{aligned} \dot{A} &= 1 - \frac{[\lambda_1 - (1-\varepsilon)F_A]P_1}{1-F_A}, \\ \nu \dot{P}_1 &= \{\lambda_1 - (1-\varepsilon)\}P_1, \\ \nu \dot{P}_2 &= (\lambda_2 - 1)P_2, \end{aligned} \tag{3.6}$$

where

$$\begin{aligned} \lambda_1 &= \frac{N}{1 - \kappa(1-N) + \frac{\varepsilon N^2}{A^2\left\{1+\sqrt{\frac{\varepsilon}{1-\kappa}}\frac{N}{A}\right\}}}, \\ \lambda_2 &= \frac{N}{1-\kappa(1-N)}, \end{aligned} \tag{3.7}$$

and N is determined from the conservation law

$$N + \sigma(P_1 + P_2) = K, \tag{3.8}$$

where the constant K is determined from the initial conditions. The additional parameters are defined by

Author's personal copy

$$\sigma = \frac{P_0}{N_0}, \quad \nu = \frac{I}{A_0 h_2}; \tag{3.9}$$

typical values of the dimensionless parameters are given in Table 4.

Summing the equations for P_1 and P_2 and ignoring the terms in $\varepsilon \ll 1$, we see that (using 3.8)

$$\nu \dot{N} \approx \frac{(1-\kappa)(N-1)(N-K)}{1-\kappa(1-N)}. \tag{3.10}$$

Because $\kappa < 1$ and since initially $N < K$, we see from this that $N \to 1$ on a time scale $O(\nu)$, essentially instantly. Let us anticipate that thereafter $N = 1 + o(\varepsilon)$; we then have

$$\lambda_1 \approx 1 - \frac{\varepsilon}{A^2}, \tag{3.11}$$

so that approximately,

$$\begin{aligned} \dot{A} &= 1 - \left[1 + \frac{\varepsilon}{1-F_A}\left(F_A - \frac{1}{A^2}\right)\right] P_1, \\ \nu \dot{P}_1 &= \varepsilon \left[1 - \frac{1}{A^2}\right] P_1. \end{aligned} \tag{3.12}$$

This essentially takes us back to the two equation model. We regain it by writing

$$A = 1 + \delta a, \quad P_1 = p, \quad t \sim \delta, \tag{3.13}$$

where we choose

$$\delta = \sqrt{\frac{\nu}{2\varepsilon}} \ll 1; \tag{3.14}$$

ignoring the small terms which remain, we regain the sawtooth model in the form

$$\begin{aligned} \dot{a} &= 1 - p, \\ \dot{p} &= ap. \end{aligned} \tag{3.15}$$

As before, we have ignored a small damping term of $O(\delta\varepsilon)$ in the a equation, thus the oscillations of the model will eventually die away.

It remains to enquire what befalls P_2 and N. We previously assumed $N = 1 + o(\varepsilon)$. Let us write

$$N = 1 + \omega n, \tag{3.16}$$

where we must determine $\omega \ll \varepsilon$. From (3.6), (3.7) and (3.8), we have (also rescaling t via 3.13)

$$-\omega \dot{n} - \dot{p} = \frac{(1-\kappa)n}{1+\kappa\omega n}[K - 1 - \sigma\omega n - \sigma p], \tag{3.17}$$

providing we choose

$$\omega = \frac{\sigma\nu}{\delta}, \tag{3.18}$$

Author's personal copy

which is indeed $\ll \varepsilon$ as assumed. Approximately,

$$n = -\frac{\dot{p}}{(1-\kappa)(K-1)}. \tag{3.19}$$

Note that since

$$P_2 \approx \frac{K-1}{\sigma} - p, \tag{3.20}$$

there is an upper bound to the maximum value of p, and thus the energy $E = \frac{1}{2}a^2 + p - \ln p$ for (3.15) cannot be larger than $(K-1)/\sigma$, and when the spikes in p cause a drop in P_2, as in Fig. 4, one can say that indeed $E \sim \dfrac{1}{\sigma}$. For Fig. 4, we specifically have $E \approx 32.7$. The dimensionless maximum of p is 36.25, while $(K-1)/\sigma = 72.5$ for $K = 2.16$ and $\sigma = 1.6 \times 10^{-2}$, which is why P_2 drops by a half in the P_1 spikes in Fig. 4.

4 Discussion

The stimulus for this work was the observation of spiking behaviour in the simple alkalinity-calcifier model, and its elaboration to the competition model by [13]. Similar spiking behaviour occurs in other oscillatory and chaotic systems (cf. [4–6]), and it is of mathematical interest to understand how such behaviour can occur in an essentially second order system.

The answer we have found is that the model can be represented in its simplest form as a conservative nonlinear oscillator with an asymmetric potential, and it is this asymmetry which promotes sawtooth oscillations and spiking, when the associated conserved energy is large.

However, the oscillations are not sustained, due to a weak damping, but it is clear that a weak forcing can maintain the oscillations. As an illustration, the forced system

$$\ddot{\theta} + V'(\theta) = \delta\left[f(t) - \dot{\theta}e^{\theta}\right] \tag{4.1}$$

(cf. 2.12) satisfies the energy equation (cf. 2.15)

$$\dot{E} = \delta\left[f(t)\dot{\theta} - \dot{\theta}^2 e^{\theta}\right], \tag{4.2}$$

and thus periodic solutions can be maintained if the average of $f\dot{\theta}$ is non-zero, i. e., if the forcing resonates with the natural frequency of the oscillation. This is essentially the situation appropriate in the ice age problem, because the Milanković forcing provides a weak signal at the resonant period of 100 ka. Omta et al. [13] conclude that the oscillations in CO_2 which are observed may thus be due to the carbonate-calcifier oscillation in the ocean. The resulting oscillations cause oscillations in dissolved CO_2, which leads to oscillations in atmospheric CO_2, and it is these which drive the ice ages.

This is an attractive scenario, but it may not be realistic. Fowler et al. [7] also studied a model in which ice sheet growth was controlled by a climate whose temperature was also linked to carbon in the ocean. Apart from the carbon species, they also included ocean calcium, phosphorus, calcium carbonate as biomass and acidity. In contrast to Omta et al., they found that the ocean carbon system was stable in practice, although the same autocatalysis was

Author's personal copy

embedded in their model. A further comparison of the two approaches would be worthwhile. However, our principal result has been the identification of the asymptotic nature of the mechanism which causes spiking and sawtooth oscillations in the carbonate-calcifier model.

Acknowledgments I acknowledge the support of the Mathematics Applications Consortium for Science and Industry (http://www.macsi.ul.ie) funded by the Science Foundation Ireland mathematics initiative grant 06/MI/005. This publication has emanated from research conducted with the financial support of Science Foundation Ireland under Grant Number: SFI/09/IN.1/I2645.

References

1. Croll, J.: On the physical cause of the change of climate during geological epochs. Phil. Mag. **4**(28), 121–137 (1864)
2. Croll, J.: Climate and Time in Their Geological Relations: a Theory of Secular Changes of the Earth's Climate. Daldy, Isbister, London (1875)
3. Crucifix, M.: Oscillations and relaxation oscillators in Pleistocene climate theory. Phil. Trans. R. Soc. A **370**, 1,140–1,165 (2012)
4. Fowler, A.C.: Approximate solution of a model of biological immune responses incorporating delay. J. Math. Biol. **13**, 23–45 (1981)
5. Fowler, A.C.: An asymptotic analysis of the logistic delay equation when the delay is large. IMA J. Appl. Math. **28**, 41–49 (1982)
6. Fowler, A., McGuinness, M.J.: A description of the Lorenz attractor at high Prandtl number. Physica **5D**, 149–182 (1982)
7. Fowler, A.C., Rickaby, R.E.M., Wolff, E.W.: Exploration of a simple model for ice ages. Int. J. Geomath. (2012). doi:10.1007/s13137-012-0040-7
8. Goldbeter, A.: Biochemical oscillations and cellular rhythms. C.U.P., Cambridge (1996)
9. Hays, J.D., Imbrie, J., Shackleton, N.J.: Variations in the Earth's orbit: pacemaker of the ice ages. Science **194**, 1,121–1,132 (1976)
10. Laskar, J., Robutel, P., Joutel, F., Gastineau, M., Correia, A.C.M., Levrard, B.: A long-term numerical solution for the insolation quantities of the Earth. Astron. Astrophys. **428**, 261–285 (2004)
11. Lisiecki, L.E. Raymo, M.E.: A Pliocene-Pleistocene stack of 57 globally distributed benthic δ^{18}O records. Paleoceanography **20**, PA1003 (2005). doi:10.1029/2004PA001071
12. Milanković, M.: Canon of Insolation and the Ice-Age Problem (Translated from German edition of 1941). Agency for Textbooks, Belgrade (1941) (1998)
13. Omta, A.W., van Voorn, G.A.K., Rickaby, R.E.M., Follows, M.J.: On the potential role of marine calcifiers in glacial-interlacial dynamics. Glob. Biogeochem Cycles (2013) (in revision)
14. Petit, J.R., Jouzel, J., Raynaud, D., Barkov, N.I., Barnola, J.-M., Basile, I., Bender, M., Chappellaz, J., Davis, M., Delaygue, G., Delmotte, M., Kotlyakov, V.M., Legrand, M., Lipenkov, V.Y., Lorius, C., Pépin, L., Ritz, C., Saltzman, E., Stievenard, M.: Climate and atmospheric history of the past 420,000 years from the Vostok ice core, Antarctica. Nature **399**, 429–436 (1999)
15. Saltzman, B.: Dynamical Paleoclimatology: Generalized Theory of Global Climate Change. Academic Press, San Diego (2002)
16. Saltzman, B., Hansen, A.R., Maasch, K.A.: The late quaternary glaciations as the response of a three-component feedback system to Earth-orbital forcing. J. Atmos. Sci. **41**, 3,380–3,389 (1984)
17. Saltzman, B., Maasch, K.A.: Carbon cycle instability as a cause of the late Pleistocene ice age oscillations: modeling the asymmetric response. Glob. Biogeochem. Cycles **2**, 177–185 (1988)
18. Saltzman, B., Maasch, K.A.: A first-order global model of late Cenozoic climatic change. II. Further analysis based on a simplification of CO_2 dynamics. Clim. Dyn. **5**, 201–210 (1991)
19. Shakun, J.D., Clark, P.U., He, F., Marcott, S.A., Mix, A.C., Liu, Z., Otto-Bliesner, B., Schmittner, A., Bard, E.: Global warming preceded by increasing carbon dioxide concentrations during the last deglaciation. Nature **484**, 49–55 (2012)